HHS Public Access

Author manuscript

Nanophotonics. Author manuscript; available in PMC 2017 November 30.

Published in final edited form as:

Nanophotonics. 2017 July ; 6(4): 647–661. doi:10.1515/nanoph-2016-0156.

Optofluidic bioanalysis: fundamentals and applications

Damla Ozcelik,
School of Engineering, University of California-Santa Cruz, 1156 High Street, Santa Cruz, CA 95064, USA

Hong Cai,
School of Engineering, University of California-Santa Cruz, 1156 High Street, Santa Cruz, CA 95064, USA

Kaelyn D. Leake,
School of Engineering, University of California-Santa Cruz, 1156 High Street, Santa Cruz, CA 95064, USA

Aaron R. Hawkins, and
ECEn Department, 459 Clyde Building, Brigham Young University, Provo, UT 84602, USA

Holger Schmidt*
School of Engineering, University of California-Santa Cruz, 1156 High Street, Santa Cruz, CA 95064, USA

Abstract

Over the past decade, optofluidics has established itself as a new and dynamic research field for exciting developments at the interface of photonics, microfluidics, and the life sciences. The strong desire for developing miniaturized bioanalytic devices and instruments, in particular, has led to novel and powerful approaches to integrating optical elements and biological fluids on the same chip-scale system. Here, we review the state-of-the-art in optofluidic research with emphasis on applications in bioanalysis and a focus on waveguide-based approaches that represent the most advanced level of integration between optics and fluidics. We discuss recent work in photonically reconfigurable devices and various application areas. We show how optofluidic approaches have been pushing the performance limits in bioanalysis, e.g. in terms of sensitivity and portability, satisfying many of the key requirements for point-of-care devices. This illustrates how the requirements for bianalysis instruments are increasingly being met by the symbiotic integration of novel photonic capabilities in a miniaturized system.

Keywords

biosensing; integrated optics; lab-on-chip; optofluidics; photonics

***Corresponding author: Holger Schmidt**, School of Engineering, University of California-Santa Cruz, 1156 High Street, Santa Cruz, CA, 95064, USA, hschmidt@soe.ucsc.edu.

Competing financial interests: The authors declare that they have no competing financial interests.

1 Introduction

The recent emergence of the new field of optofluidics has led to a surge in activities aimed at harnessing light-matter interactions in integrated devices with unprecedented and/or dramatically improved capabilities. In its earliest incarnations [1, 2], optofluidics was envisioned to lead to a new class of reconfigurable devices such as lasers [3], new manipulation techniques for nanoparticles and microparticles [4], and new biophotonic applications such as optofluidic microscopy [5]. In addition, it was speculated that full chip-scale optofluidic systems would be built in modular fashion from different layers for light guiding, fluid handling, and control, respectively [1]. This original vision has largely held true, although recent reviews show that applications of this technology have gravitated away from classical optical communication devices toward biological and chemical sensing – in other words, away from emphasizing the photonic reconfigurability toward focusing on the contents of the fluids that made up the device [6–9]. Moreover, additional potential application areas such as energy harvesting were identified and a number of topical reviews on various aspects of the field are now available [10–16]. Bioanalysis applications have received so much attention due to the much larger efforts that have been initiated in the lab-on-chip community for creating miniaturized instruments that help deal with the ever-increasing need for biomedical testing. Infectious diseases, for example, are constantly threatening humans and are among the leading causes of deaths across the globe [17]. Integrated virus detection systems need to fulfill several requirements to satisfy the needs of the medical community. These include low limits of detection of viral or bacterial loads, large dynamic range, and the ability for multiplex detection of multiple targets at once [18]. Other secondary factors, such as time-to-result, cost, ease-of-use, and experimental complexity, also need to be considered, and the latest optofluidic solutions can now address all these challenges successfully. Similarly, recent progress in optofluidic particle manipulation and trapping promises another type of powerful and easy-to-use instrument for use in laboratory and clinical diagnostics. It is, therefore, the perfect time to pause and take stock of the most recent trends and achievements in optofluidics. In this review, we emphasize optofluidic approaches that involve optical waveguides, either planar or fiber-based, as this provides the ultimate level of integration between optical and fluidic elements and functions. We will first highlight fundamental work in devices that implement canonical optofluidic principles and functions. (For an in-depth review of the scientific underpinnings of micro-fluidic and integrated optics, see [8]). Developments in a wide range of optically reconfigurable photonic devices and their incorporation in chip-scale platforms are presented. Notably, we will describe several examples of “hybrid integration” that rely on combinations of different layers and functionalities following the original spirit of optofluidic integration. We will then discuss current areas of applications with a focus on two areas: particle manipulation and bioanalysis. We will see that the performance of optofluidic devices, for example, in terms of sensitivity at the single particle limit down to single nucleic acids and compatibility with portable carrier platforms such as smartphones, has reached levels that are highly competitive with existing commercial products. We highlight how practical needs for a bioanalytic application drive the photonic device design and conclude with an outlook to possible future developments.

2 Reconfigurable optofluidic devices and systems

The fact that liquid or gaseous fluids are nonsolid enables their movement and even complete replacement using external pressure or other means. This distinctive property is the driver behind creating reconfigurable photonic devices, which was an early focus of optofluidics [1, 2]. One natural choice for such a device is a reconfigurable on-chip light source. Consequently, optofluidic lasers were developed early on, demonstrating key hallmarks of reconfiguration. These include the use of organic dyes in microchannels as the gain medium [19, 20] or the dynamic tuning of the laser emission wavelength using mechanical deformation of the microfluidic chip [21, 22]. More recently, the attention in optofluidic light sources has shifted toward new, biologically inspired gain media. For example, Wu et al. [23] used luciferin, a light-emitting molecule produced by many organisms, to show that photonic devices can be created using biosynthesized materials as the active medium with possible applications in intracavity sensing. It was even possible to create a laser based on fluorescence resonance energy transfer (FRET) using luciferin and rhodamine 6G molecules as FRET donors and acceptors, respectively. In a similar vein, Figure 1A illustrates the demonstration of using vitamin B2-doped gelatin films as gain media for distributed feedback (DFB) lasers [24]. Here, it was shown that the deposition of an optically active layer composed of gelatin from porcine containing riboflavin at 1.3 mm concentration is compatible with the fabrication workflow of an optofluidic laser. DFB grating was designed to fulfill the Bragg resonance condition in second order to achieve vertical emission. When optically pumped with an external parametric oscillator, the device exhibited single-mode emission at 543 nm for a grating period of 368 nm.

Using biomolecules as active media can provide additional novel features as demonstrated by reversible switching of the lasing wavelength using DNA Holliday junctions in an optofluidic ring resonator (OFRR) based on the chemical environment [25]. Most recently, the use of green fluorescent proteins within a single cell embedded in an external microcavity was shown to create lasing action while keeping the cell alive [26], and lasing in blood was also shown [27]. The latter example is illustrated in Figure 1B. The left image shows schematically the excitation geometry for optical pumping of indocyanine green (ICG) dye flowing through an OFRR capillary. Here, ICG in micromolar, biocompatible concentration binds to low-density lipoproteins (LDL). Figure 1B (right) shows the appearance of a clear laser threshold under optical pumping with an external parametric oscillator. A more extensive discussion of the current state and potential of such bioinspired optofluidic lasers can be found in [28].

Another canonical element that is used in photonic devices is a resonator that typically provides a narrow-band optical response whose changes can be used for sensing applications. In the past, various types of OFRRs, both planar and capillary-based, were demonstrated [6, 29, 30]. These were used for constructing lasers, particle traps and sorters, and interference devices [29–31]. Freestanding high-Q microcavities were also demonstrated to show highly sensitive resonances in an aqueous environment with possible applications for biosensing [32]. A recent example for this approach is the use of nanoporous polymer ring resonators that allow molecular targets to penetrate into the resonator volume for increased light-target interaction and increased sensitivity [33]. A more recent trend in the

resonator arena is the combination of optofluidics and (cavity) optomechanics, which focuses on the interaction of light with mechanically resonant structures [34]. The optomechanic properties of microfluidic resonators have been studied [35, 36], and their use as sensors for pressure, inertia, mass, and temperature was investigated. For example, Kim and Fan demonstrated that vibrational frequency changes in microfluidic optomechanical ring resonators can be translated into mass detection limits as small as 83 pg/mm^2 [37].

A third representative area of reconfigurable optical devices is that of optofluidic lenses and light shaping. Early work included liquid microlenses based on electrowetting [38], lenses in liquid-core liquid-cladding waveguide channels [39], and tunable gradient refractive index (RI) lenses [40]. More recent examples are the demonstration of an optofluidic bi-concave lenses that allow tuning a light beam from focusing to diverging [41] and a tunable microlens that is controlled via an active pressure of an air-liquid interface [42]. A very innovative development is the demonstration of an optofluidic light splitter based on transformation optics [43]. A bidirectional gradient index is created by advection in a liquid flow stream. The medium then has an inhomogeneous RI distribution whose properties can be modeled via transformation optics. The power of this approach was demonstrated by creating a Y-splitter that can be operated at splitting angles up to 30°, which can be asymmetric and reconfigurable by tuning the fluid and flow properties.

As individual optofluidic elements and devices have reached higher performance levels and maturity, reconfigurability on the system instead of the device level has recently started to garner more attention. System-level reconfigurability is enabled by some form of different elements. In its most direct form, this involves the hybrid integration of two or more chips, each optimized for a different purpose and often made with different materials and fabrication processes. Parks et al. [44] reported the first example of hybrid optofluidic integration by combining polydimethylsiloxane (PDMS) microfluidic chips with silicon-based optofluidic waveguide chips for implementing key sample processing steps with sensitive optical particle detection, respectively. Demonstrated capabilities included mixing, size filtering, and fluidic distribution of dielectric microbeads into multiple detection channels exclusively using pressure-based flow in the microfluidic device layer. System reconfigurability was implemented using nonpermanent connections between the different device layers. A similar approach was demonstrated by Testa et al. [45] who also created a 3D system by combining PDMS and silicon chips and demonstrating fluorescence detection of dyes at nanomolar concentrations. Subsequently, Parks et al. [46] further expanded on the capabilities of the optofluidic system using active valve control in the microfluidic layer. Specifically, interconnected lifting-gate microvalves (“automata” [47, 48]) were used to create a network of submicroliter volumes that can be activated and transported across the chip using pneumatic control. This was used to implement a solid-phase extraction assay to selectively bind and label oligomers with an Ebola virus sequence to magnetic microbeads, which can then be detected on a connected optofluidic chip [49]. System-level integration can be taken even further if optofluidic elements are connected to larger, highly functional elements. This is nicely illustrated by the increasing number of reports that use attachments to portable cellphones to accomplish a particular task [50–53]. Clearly, the growing efforts on the system and instrument level show that the commercialization of optofluidic systems is imminent.

3 Applications

Because nonsolid media are at the core of optofluidics, applications can be conceived around both gases and liquids. Indeed, several avenues involving gases and vapors such as on-chip atomic spectroscopy [54], metrology and quantum interference [55] along with chemical sensors such as gas chromatographs [56, 57] and others have successfully been taken. However, the largest potential and ostensibly the biggest markets are in the life sciences, which typically require the analysis of liquid media and their components. For the remaining portion of the review, we will look at two applications of optofluidics with implications for the life sciences. The first involves the optofluidic manipulation of microparticles and nanoparticles, i.e. controlling particle location using physical forces via pushing, trapping, and/or sorting, and the second is optofluidic particle sensing, i.e. detecting the presence and nature of a moving or immobilized particle, which has a tremendous potential for diagnostic tests and instruments.

4 Optofluidic particle manipulation

The ability to use optical forces to physically manipulate particles ranging from dielectric microbeads to single nanoscale biomolecules on a chip has an been an integral part of optofluidics since the early days when trap-assisted optical switches [58, 59] and quantum dot-based optofluidic memories [60] were considered. In subsequent years, efforts increasingly focused on manipulating particles of varying size and type using on-chip waveguide structures on which we will focus here.

Optical particle manipulation is possible because photons carry a linear momentum of $p = h/l$, where h is Planck's constant and l is the wavelength. As a light beam interacts with a particle via reflection, refraction, or absorption, the photon momentum is changed, resulting in an optical force $F_{opt} = dp_{tot}/dt$ on the particle. This force can be used to control the motion of the particle. We distinguish two components of the optical force as shown in Figure 2, which shows a dielectric particle subjected to a propagating light beam with an inhomogeneous (here Gaussian) intensity profile.

The scattering force F_S acts along the propagation direction of the light beam, and its magnitude is proportional to the amount of power (intensity) that hits the particle. The gradient force F_G occurs in beams with spatially varying intensity profiles, and its magnitude is proportional to the local power (intensity) gradient. For most practical cases (the RI of particle is larger than the index of surrounding medium), the gradient force pulls the object to high-intensity regions of the beam. Both types of force are present in integrated waveguide structures, and one of the attractive motivations for using waveguides for particle manipulation is the possibility to precisely control the spatial dependence of these forces with proper fabrication. Optofluidic implementations of these principles can be done in a variety of ways, involving either solid-core or liquid-core waveguides. In the former approach, light is guided by total internal reflection in a high index core. Light-particle interactions take place either near the core surface via the evanescent tail of the guided mode or over a short channel segment in which the light is not guided. Surface wave optical

manipulation is implemented using both linear waveguide-based and microresonator-based devices.

Evanescent waves on the surface of a planar photonic device have been used for the optical manipulation of microparticles/nanoparticles as early as 1996 [61]. The optical gradient force can be maximized by ensuring high RI contrast between waveguides and the surroundings. For example, a silicon nitride (SiN)-water interface with an RI contrast of ~2/1.33 produces up ~20 times higher optical forces on 2 mm microparticles than a glass waveguide [62]. Such evanescent fields can be used for the optical manipulation of particles in the tens of nanometer range [63, 64], in which conventional optical tweezers are limited by the diffraction limit. Thanks to soft lithography technology, planar waveguides on a photonic chip can be seamlessly integrated with microfluidic channels. For example, SU8 (RI ~ 1.57) waveguides were used to optically manipulate microparticles delivered by a microfluidic channel over the top of the waveguides [65].

A logical extension of moving or trapping a particle on a straight waveguide is to split the waveguide into two output ports to form a Y-junction. By simply adjusting the input-coupling fiber positions to differentiate the power between the output ports, 6 mm polystyrene particles can be trapped by the input waveguide and routed to the preferred output port with higher guided power [66]. Moreover, 1 × 2 splitters have also been implemented using multimode interference (MMI) waveguides [67, 68]. Here, the power ratio between the two output ports can be tuned by wavelength and various particle splitting ratios were observed [69, 70]. Another clever way to transfer power, and concomitantly microspheres, between waveguides is to place two waveguides in close proximity. Optical power is then evanescently coupled back and forth between the input-waveguide and the coupled waveguide. By the proper design of the coupling gap and coupling length, one can achieve different output power ratios. Optical manipulation and lateral transfer of 10 mm polystyrene spheres was achieved on such a waveguide-based directional coupler using the gradient force across the small gap at a certain interaction length [70]. Because the coupling length also depends on the input laser wavelength, the coupling transfer efficiency can again be controlled by tuning the input laser wavelength. By introducing a structural perturbation near the junction of the coupling region, microparticle sorting on directional couplers was demonstrated [71].

The transfer of optical powers via close proximity of two waveguide structures can be extended to microring resonators coupled to a bus waveguide. Microresonators are attractive because they can store strong cavity fields, which result in stronger gradient and scattering forces. Thus, the field enhancement inside the resonator can enable efficient optical manipulation while keeping the input laser power relatively low. Microresonators can also greatly expand the functionalities of waveguide-based microparticle/nanoparticle routing and sorting. The first planar resonator-based optical manipulation was reported by Mandal et al. [72] using a photonic crystal cavity in 2010. A schematic view and a scanning electron microscopy (SEM) image of this seminal structure are shown in Figure 3A.

Photonic crystal cavities are formed by introducing well-defined defects into waveguiding slabs whose RI is modulated by a group of submicron-scale periodic air holes. The defects

in the photonic crystal act as optical resonators or cavities by creating a pass-band in the photonic band gap. Small mode volume with large optical field enhancement can be achieved inside the cavities. The photonic resonator can be evanescently coupled to a single-mode waveguide. In this example, resonators and waveguides were fabricated from 250-nm-thick silicon on silicon-on-insulator wafers using electron beam lithography. Light was coupled into the bus waveguide using an infrared erbium-doped fiber amplifier. The fluidic interface was provided by bonding PDMS microfluidic channels (120 μm wide and 5 μm tall) to the chips using plasma treatment and controlling fluid flow via syringe pumps.

When the photonic crystal cavity is resonant with the optical wavelength, a strong standing wave is formed inside the cavity, which provides a 3D stationary potential well to confine microparticles/nanoparticles, as shown in Figure 3B, indicating maximum optical (gradient) forces on the 1D resonator. Figure 3C shows the example of a trapped 500 nm polystyrene microsphere. The input light is initially tuned to the resonant wavelength, causing a particle to move along the waveguide. When it reached the resonator, the lateral gradient force pulled it toward the resonator center. This demonstration showed the integration of nanofabricated waveguide structures with a microfluidic environment and the use of optical trapping for the subsequent identification or analysis of a microscale or nanoscale particle down to 48 nm size.

Large biological bacteria such as *Bacillus subtilis* and *Escherichia coli* were successfully trapped using a different kind of 1D silicon photonic crystal cavity [73]. With similar design on an SiN platform using 1064 nm laser wavelength, 22-nm-sized polymer particles were trapped steadily [74]. More recently, trapping of submicron-sized particles was demonstrated using 2D hollow photonic crystal cavities on a patterned silicon substrate [75]. This approach also allowed for detecting the presence of a particle in the trap by monitoring the resonance wavelength of the device.

Circular and disk-shaped resonators are even more popular in silicon photonics than linear photonic crystal resonators [76–80]. The spectral selectivity and field enhancement inside of the resonators enable microresonators to be a versatile and powerful building block for tunable optical manipulation devices/circuits. For example, a microring resonator on resonance provides the same trapping capability as the linear input bus waveguide but with an order of magnitude lower input laser power [30]. Microparticles trapped on the ring resonator traveled around the microring at hundreds of micrometers per second, producing periodic revolutions at a few hertz with highly accurate positioning. By coupling a microresonator to two bus waveguides, more elaborate three-port particle manipulation devices such as an add-drop filter have been realized [81, 82]. Alternatively, multiple resonators with different resonance frequencies can be used to route and store dielectric microparticles on different microrings [83].

Microdisk resonators whose surface comprises the entire disk provide a wider trapping area than a microring, possibly allowing for parallel processing in optical manipulation. Microdisk resonators usually support multiple whispering gallery modes (WGM), which exhibit multiple mode-field maxima (MFM) along the radial direction, resulting in multiple tracks for particle trapping [84]. Most recently, researchers have begun using the trapping

approaches that were developed using inorganic microparticles for the active manipulation of biological objects such as nucleic acids [85], bacteria [86], and proteins [87].

The second conceptual approach to optofluidic particle manipulations is based on the use of hollow-core or liquid-core waveguides to guide light and particles through the same channel. This has the advantage that particles experience the full intensity of the optical field over extended distances. Here, the main challenge lies in creating efficient optical confinement in a low-index nonsolid core and developing an interface to deliver light and liquid to the interaction region. A number of liquid-core waveguide types including leaky waveguides [88], porous cladding waveguides [89], slot waveguides [90], liquid-liquid [91], and liquid-air waveguides [92], hollow-core photonic crystal fibers (HC-PCF) [93], and liquid-core antiresonant reflecting optical waveguides (LC-ARROWs) [94–96] have been developed for this purpose.

The earliest demonstration of moving a particle inside a waveguide was reported in 1995 by Renn et al. [97] who used a laser guided through a hollow core fiber to move rubidium (Rb) atoms along the interior of the fiber. The propulsion along the fiber was due to the scattering force, whereas the atoms were drawn to the center of the waveguide by the gradient force generated by the guided optical mode. In 2007, Mandal and Erickson pushed 3 μm polystyrene beads in a liquid-core PCF with a core diameter of 20 μm. By shining a 488 nm argon laser upward particles could be stopped by balancing gravity with the scattering force and the gradient force due to fiber loss [98]. Over the past decade, several approaches to trapping particles in liquid-filled channels were developed, starting with a dual-beam trap made from opposing diverging beams that cross a fluidic channel in between solid waveguides [99]. In 2009, gradient force-induced trapping of 75 nm polystyrene beads and L-DNA into nanoscale slot waveguides was reported [100]. Several methods for particle manipulation were proposed and demonstrated in LC-ARROWs in which the optical confinement in a low-index liquid is created using dielectric layers of alternating materials that are antiresonant, i.e. highly reflective, for the transverse wavevector component of a propagating mode [101]. These examples are illustrated in Figure 4, where blue channels depict the liquid-core waveguides in which particles are being physically manipulated and gray and green colors indicate solid-core waveguides interfacing with these channels.

A single beam in the liquid-core channel exerts a scattering force along the propagation direction and gradient forces toward the center of the confined mode. This allowed for efficient transport of 1 mm dielectric spheres in the channel and the extraction of the waveguide loss and mode profiles (Figure 4A) [102]. If two opposing beams are used as shown in Figure 4B, a loss-based dual-beam trap for the confinement of single [103] or multiple [104] particles is created. Orthogonally intersecting optical beams can also be used for confining a particle [105]. The on-chip equivalent of an electro-optical (ABEL) trap [106] is created if fluorescence is excited via two offset intersecting solid-core waveguides similar to Figure 4B and then used to identify the direction of particle movement in the channel. Subsequently, an electrical voltage can be used to apply electrical forces that compensate for the particle drifting away from the waveguide intersection region. This was demonstrated using dielectric spheres as small as 100 nm and single *E. coli* bacterium. Using a wide MMI waveguide, multiple trapping spots can be created in the fluidic channel

(Figure 4C). This was used to trap multiple 3 mm polystyrene particles simultaneously and to deliberately move a particle between trapping locations by modulating the trapping spot location with the wavelength of the trapping beam [107]. Finally, highly efficient microparticle sorting was demonstrated in the H-shaped liquid-core channel layout shown in Figure 4D [108]. In this case, balancing the size-dependent optical force with an independent flow speed provides good selectivity.

Recently, Bellini et al. [109] fabricated an optofluidic-fused silica glass-based chip using a femtosecond laser to trap and stretch a single red blood cell (RBC). The chip featured two optical waveguides that intersect with a microfluidic channel. The trapping and stretching was done with a 1070 nm laser coupled into a fiber and then split between the two waveguides. Each side's power can be independently tuned by adjusting variable optical attenuators that allow the cell position to be changed. Cell elongations up to 25%, which exceed the elastic limit of the cell, were achieved.

5 Optofluidic biosensing

As discussed above, biosensing is the largest application area for optofluidic devices at the moment, focusing on the detection and identification of biological targets or parts thereof [110]. Initially, only imaging using an optofluidic microscope was considered as a biosensing application [5]. Interest quickly spread to biomarker detection on the cellular and molecular level particularly because of the natural overlap and synergy with the lab-on-chip community, which focused predominantly on the miniaturization of sample preparation and nonoptical sensing modalities.

A lot of initial activity developed around surface-enhanced Raman scattering (SERS) analysis in which the wavelength shift of photons due to inelastic scattering from characteristic molecular vibrations is detected [111–114]. Recent activities in this field include the development of nanoporous SERS microsystems [115], inkjet printed SERS substrates [116], and point-of-care detection and real-time monitoring of drugs with an integrated SERS sensor [117].

A second area to which significant efforts have been devoted is the development of surface plasmon resonance (SPR) sensors [118] and other plasmonic devices. Generally, these devices rely on detecting wavelength shifts in narrow SPRs upon binding of a target analyte. If this binding process is target specific, identification can take place without a fluorescent label. Commercial SPR instruments for applications in antibody detection, binding kinetic analysis, or epitope mapping exist (e.g. GE Biacore), but they typically rely on prism-based approaches (Kretschmann configuration) to optically excite surface plasmon polaritons (SPP), which is not ideal for miniaturization and low-cost production. Recently, numerous optofluidic implementations of this principle for the detection of viruses and other targets have been demonstrated [119–129]. One recent example that elegantly combines nanophotonic principles with biological sample analysis is an interferometric biosensor that relies on a nanostructured slit-groove design in which alternating slits and grooves (~100 nm width and 70 nm depth) are defined by a focused ion beam in a 350-nm-thick silver film on a glass substrate (Figure 5A) [130]. When illuminated from the bottom with TM-polarized

light, SPPs are launched at the slit and propagate toward the grooves. Light reflected from the grooves interferes with light directly transmitted through the slit as shown in Figure 5B. The transmission intensity that is produced based on this interference depends sensitively on the RI on the surface, which changes based on target adsorption. This approach is ideal for creating small footprint sensors. The device was successfully applied to detect proteins, as illustrated by the anti-BSA to BSA binding on the surface in Figure 5C.

Resonance linewidths as low as 7 nm and an RI resolution of 10^{-5} RIU were achieved. Moreover, an array of these sensors was used to implement real-time multiplex sensing. Moving increasingly toward instruments that are viable in the field, Cetin et al. [131] recently reported a handheld device that uses plasmonic microarrays coupled with a lens-free imaging system for high-throughput multiplex protein detection. Additional future possibilities arise from the combination with more sensitive materials as illustrated by the recent demonstration of protein monolayer detection relying on the tight light confinement in graphene membranes [132].

Biosensing modalities such as SERS and SPR that are based on surface-bound optical techniques have shown to be sensitive, but they do not usually reach the single biomolecule limit, except in extreme cases requiring extraordinary fabrication and calibration precision. One way to reach this ultimate sensitivity limit is to use wide-field imaging-based methods, where the optical readout path is not integrated on the microchip but incorporated with standard, even portable, imaging systems such as smartphone cameras [51, 133]. More broadly, due to its ubiquity and built-in imaging features, the smartphone has been emerging as a desirable component of a handheld optofluidic analysis system. Other examples include rapid blood analysis [50], a diagnostic test reader platform [52], and a high-throughput instrument for the detection of single H1N1 viral particles [134]. Figure 6 shows a particularly powerful, recent approach that involves the use of biocompatible wetting films to form liquid nanolenses by self-assembly. In this case, liquid nanolenses are formed by a biocompatible buffer liquid that assembles around nanoparticles and is stable for more than 1 h. With their help, individual nanoparticles can be identified by light scattering as the nanolens acts as a spatial phase mask that produces a holographic diffraction pattern. Figure 6A shows the holographic image produced by individual H1N1 viruses on the surface of the lens array selected from a large (20.5 mm^2) image. The signal can be further processed using a phase reconstruction algorithm to yield the location of the viruses with high accuracy as seen in Figure 6B. This illustrates how effective signal processing algorithms can produce images with quality comparable to standard, bulk microscopy equipment.

The utility of smartphone-based portable system is now being put to the test. In 2014, Jiang et al. [53] reported the integration of solar-powered polymerase chain reaction (PCR) amplification for nucleic acid detection with microfluidics to minimize the need for external power sources in the field and/or low-resource settings. Figure 6C shows a photograph of this portable system and its components, including the microfluidic chip on which the PCR process is implemented and the smartphone used for optical analysis. Figure 6D shows simulations of the temperature distribution across the microfluidic channel disk, which shows that the temperature range required for implementing all steps of a PCR cycle can be reached over only 1.5 cm. It was also shown that a standard cell phone battery was able to

provide up to 70 h of power to the system, which was successfully used to detect herpesvirus in skin biopsies via smartphone-based fluorescence detection.

Methods based on the specific binding of a target analyte to a surface are common but do face some challenges in the context of miniaturization. These include insufficient limit of detection due to the ineffective transport of target particles to the binding sites, nonspecific binding, limited dynamic range, and surface deterioration. If optical readout is desired, typically the evanescent field penetrating from a solid waveguide surface into the analyte space must be used, which is inherently inefficient. Optical sensing of biomarkers with both high sensitivity and wide dynamic range can be accomplished by detecting targets in flow, similar in spirit to a flow cytometer for the investigation of cells by light scattering, fluorescence, and absorption as they flow by one or more laser sources. This approach all but eliminates the challenges described above. An intermediate step between flow- and surface-based optofluidic biosensing is the OFRR [113] – a glass capillary through which analytes can flow and whose walls sustain WGM. These ring resonator frequencies can be monitored with an adjacent optical fiber and indicate target binding or proximity to the capillary surface via a spectral shift. Low limits of detection and large, strongly sublinear dynamic range for bacteriophage detection were demonstrated. Another recent example for semi-integrated, capillary-based analysis in flow is the detection of 20 nm dielectric particles and single, 26 nm cowpea chlorotic mottle virus (CCMV) virions in single-mode silica fiber having a subwavelength, nanofluidic channel by illuminating the targets along the fiber and collecting scattered light with an objective from the side [135].

A complete transition to on-chip flow-based optical biosensing calls for the use of integrated, planar waveguides for light delivery and/or collection. As early as 2004, Lien et al. [136] reported the development of monolithically integrated buried-channel waveguides for exciting dielectric microspheres in a fluidic channel followed by reports of their use for microbead detection in an array arrangement for enhanced signal-to-noise ratio (SNR) [137]. Subsequently, Bliss et al. [138] demonstrated the fabrication of PDMS waveguides for electrophoretic separation and detection of a BK virus PCR product on an optofluidic chip. Over the past few years, a number of liquid-core waveguide types have been constructed that allow for efficient optical interactions and light guiding in the fluidic channels themselves. Specifically, hollow-core ARROWs have been developed [139, 140]. Alternating dielectric layers surrounding a nonsolid core can enable low-loss light propagation by choosing the appropriate thicknesses for light confinement [101]. These hollow-core ARROWs can be interfaced lithographically with standard solid-core ARROWs to form 2D photonic networks for advanced biosensing [140, 141]. The single particle fluorescence detection can be reached because intersecting ARROWs create optical excitation/detection volumes on the order of ~10 fl, slightly larger than that of commercial scanning confocal microscopes [142–144]. This concept is illustrated in Figure 7A, where a beam guided by a solid-core waveguide (light gray) is shown to cross a fluidic channel, exciting targets that are flowing through this optical excitation region.

In addition, multiple steps to optimize light transport and interfaces were taken, including the use of low fluorescent cladding materials [145], thermal annealing of the chips [146], and optimization of waveguide intersection regions [147]. As a result, this approach has

recently enabled digital detection, i.e. direct counting, of single biomarkers such as viral nucleic acids and whole virus particles. Strain-specific detection of nucleic acids from Zaire Ebola virus from clinical samples has been demonstrated in optofluidic ARROW chips with a limit of detection of 0.2 pfu/ml and a dynamic range of 13 orders of magnitude (Figure 7B) [49]. This suggests the possibility to eliminate the need for nucleic acid amplification altogether with its requirements on sample processing, reagents, and potential error sources. Moreover, ARROWs were recently shown to enable a new multiplexing technique with enhanced SNR based on wavelength division multiplexing [148]. Using a multimode interferometer waveguide [31, 68] section to intersect the fluidic channel, color-dependent spatial excitation patterns are generated that lead to multipeak signals in the time domain as a fluorescent target flows past this excitation region. Figure 7C shows a schematic illustration of this excitation configuration along with the excitation patterns created by three colors in a dye-filled channel, showing 6, 7, and 9 spots, respectively. This transformation of spectral information into a spatial pattern allows to distinguish multiple targets labeled with different (combinations of) dyes by the number and spacing of the peaks in the detected signal (Figure 7D). This technique was able to discriminate between three influenza subtypes with single virus sensitivity and can be extended to creating different spot patterns in multiple fluidic channels for increasing throughput or the level of multiplexing. The fact that MMI waveguides result in well-defined spot patterns with equal distances allows for taking advantage of the SNR enhancement techniques that have been demonstrated using well-defined spot patterns [136, 149, 150]. Essentially, the fact that the temporal signal created by a target particle is determined by the physical spot pattern allows for signal processing methods to be applied to the detected time trace. The efficiency of this approach for MMI-based particle detection on an ARROW chip and exponential SNR improvement with the number of spots was recently demonstrated [148, 151]. Planar integration of the optical elements required for sensing has additional advantages, particularly in the context of hybrid integration. Silicon-based ARROW devices have successfully been combined with PDMS microfluidic chips to incorporate sample processing steps as described above [44–46, 49]. Moreover, their capabilities have also been expanded toward dual electro-optical detection of single nanoparticles by incorporating solid-state nanopores on the same chip. Nanopore-based electrical sensing is one of the leading candidates for next-generation sequencing and relies on the identification of a target particle based on the change in ionic current it creates as it passes through a nanoscale opening in a membrane [152]. Nanopores in solid-state membranes such as SiN have the advantage that their size and shape can be defined over a wide range and thus adapted to a specific nanoparticle. Successful integration of a nanopore in a silicon-based ARROW chip was demonstrated a few years ago, but recently this approach was combined with the aforementioned single particle optical detection to implement dual-mode correlated sensing of individual nanoparticles such as DNAs and virus particles [153–155]. This shows that optofluidic biosensing can be integrated and advanced further by adding other detection modalities. Finally, it has recently been shown that both micro-valve-based particle handling and optical sensing can be combined in a single PDMS chip relying on lifting-gate valves and integrated waveguides [156]. This allows for taking advantage of the flexible nature of PDMS to create reconfigurable photonic elements such as MMIs and for designing the microvalves themselves as movable waveguide segments. Such “lightvalves” may form the basis of

future, large reconfigurable optofluidic systems in the spirit of the original vision for the field.

6 Outlook

We have reviewed the current state of optofluidics in the context of the field's relatively young history. The field initially focused on demonstrations of canonical photonic devices that incorporate and take advantage of nonsolid media to provide reconfiguration. Most photonic elements can be implemented using an optofluidic approach, although an electrically pumped, chip-scale optofluidic laser source has remained elusive. Much of the current research focuses on ever closer connections between optical devices and biological substances as well as on the commercialization of proven optofluidic approaches to biological and chemical sensing. The full integration of sensing and sample preparation steps in a single system has taken center stage, be it via hybrid integration of dedicated chips or by developing interfaces with a full-fledged instrument such as a smartphone. In the future, even more advanced integration, particularly with integrated electronic circuits for the control of the optofluidic system and reporting and analyzing its output, is sure to come into focus. In recent years, optofluidic devices and instruments have started making their way into commercial products, mostly via startup companies. As these products mature, a clear-cut comparison to established products that are not only defined by their underlying technology but also other constraints such as packaging and fabrication costs will emerge. At the same time, new research ideas for uniting photonics and microfluidic are coming to the fore, ensuring lasting vibrancy and excitement.

Acknowledgments

This work was supported by the NIH under grants 4R33AI100229 and 1R01AI116989, the NSF under grants CBET-1159453 and CBET-1159423, and the W.M. Keck Center for Nanoscale Optofluidics at University of California-Santa Cruz.

References

1. Psaltis D, Quake SR, Yang C. Developing optofluidic technology through the fusion of microfluidics and optics. Nature. 2006; 442:381. [PubMed: 16871205]
2. Monat C, Domachuk P, Eggleton BJ. Integrated optofluidics: a new river of light. Nat Photonics. 2007; 1:106.
3. Balslev S, Kristensen A. Microfluidic single-mode laser using high-order Bragg grating and antiguiding segments. Opt Express. 2005; 13:344–51. [PubMed: 19488359]
4. Grier DG. A revolution in optical manipulation. Nature. 2003; 424:810–6. [PubMed: 12917694]
5. Heng X, Erickson D, Baugh LR, Yaqoob Z, Sternberg PW, Psaltis D, et al. Optofluidic microscopy – a method for implementing a high resolution optical microscope on a chip. Lab Chip. 2006; 6:1274–76. [PubMed: 17102839]
6. Fan X, White IM. Optofluidic microsystems for chemical and biological analysis. Nat Photonics. 2011; 5:591–607. [PubMed: 22059090]
7. Schmidt H, Hawkins AR. The photonic integration of non-solid media using optofluidics. Nat Photonics. 2011; 5:598–604.
8. Hawkins, AR., Schmidt, H. Handbook of Optofluidics. CRC Press; 2010.
9. Fainman, Y., Lee, LP., Psaltis, D., Yang, C. Optofluidics: Fundamentals, Devices, and Applications. McGraw-Hill; 2009.

10. Erickson D, Sinton D, Psaltis D. Optofluidics for energy applications. Nat Photonics. 2011; 5:583–90.
11. Rodriguez CA, Modestino MA, Psaltis D, Moser C. Design and cost considerations for practical solar-hydrogen generators. Energy Environ Sci. 2014; 7:3828–35.
12. Song W, Psaltis D. Electrically tunable optofluidic light switch for reconfigurable solar lighting. Lab Chip. 2013; 13:2708–13. [PubMed: 23652728]
13. Psaltis D, Vasdekis AE, Choi JW. Optofluidics of plants. APL Photonics. 2016; 1:20901.
14. Saad Ahsan S, Gumus A, Erickson D. Redox mediated photocatalytic water-splitting in optofluidic microreactors. Lab Chip. 2013; 13:409–14. [PubMed: 23223889]
15. Eunjung Jung E, Kalontarov M, Doud DFR, Ooms MD, Angenent LT, Sinton D, et al. Slab waveguide photobioreactors for microalgae based biofuel production. Lab Chip. 2012; 12:3740–5. [PubMed: 22824859]
16. Ahsan SS, Gumus A, Erickson D. Stacked waveguide reactors with gradient embedded scatterers for high-capacity water cleaning. Opt Express. 2015; 23:A1664–71. [PubMed: 26698812]
17. WHO. The Top 10 Causes of Death. Available at http://www.who.int/mediacentre/factsheets/fs310/en/. Accessed August 31, 2016.
18. Kuypers J, Wright N, Morrow R. Evaluation of quantitative and type-specific real-time RT-PCR assays for detection of respiratory syncytial virus in respiratory specimens from children. J Clin Virol. 2004; 31:123–9. [PubMed: 15364268]
19. Vezenov DV, Mayers BT, Conroy RS, et al. A low-threshold, high-efficiency microfluidic waveguide laser. J Am Chem Soc. 2005; 127:8952–3. [PubMed: 15969563]
20. Helbo B, Kragh S, Kjeldsen BG, Reimers JL, Kristensen A. Investigation of the dye concentration influence on the lasing wavelength and threshold for a microfluidic dye laser. Sens Actuators A Phys. 2004; 111:21–5.
21. Li Z, Zhang Z, Scherer A, Psaltis D. Mechanically tunable optofluidic distributed feedback dye laser. Opt Express. 2006; 14:10494–9. [PubMed: 19529450]
22. Song W, Psaltis D. Pneumatically tunable optofluidic dye laser. Appl Phys Lett. 2010; 96:81101.
23. Wu X, Chen Q, Sun Y, Fan X. Bio-inspired optofluidic lasers with luciferin. Appl Phys Lett. 2013; 102:203706.
24. Vannahme C, Maier-Flaig F, Lemmer U, Kristensen A. Single-mode biological distributed feedback laser. Lab Chip. 2013; 13:2675–8. [PubMed: 23532260]
25. Zhang X, Lee W, Fan X. Bio-switchable optofluidic lasers based on DNA Holliday junctions. Lab Chip. 2012; 12:3673–5. [PubMed: 22790530]
26. Gather MC, Yun SH. Single-cell biological lasers. Nat Photonics. 2011; 5:406–10.
27. Chen Y-C, Chen Q, Fan X. Lasing in blood. Optica. 2016; 3:809–15.
28. Fan X, Yun S-H. The potential of optofluidic biolasers. Nat Methods. 2014; 11:141–7. [PubMed: 24481219]
29. Yang AJH, Erickson D. Optofluidic ring resonator switch for optical particle transport. Lab Chip. 2010; 10:769–74. [PubMed: 20221566]
30. Lin S, Schonbrun E, Crozier K. Optical manipulation with planar silicon microring resonators. Nano Lett. 2010; 10:2408–11. [PubMed: 20545333]
31. Testa G, Huang Y, Sarro PM, Zeni L, Bernini R. Integrated silicon optofluidic ring resonator. Appl Phys Lett. 2010; 97:131110.
32. Armani AM, Kulkarni RP, Fraser SE, Flagan RC, Vahala KJ. Label-free single-molecule detection with optical microcavities. Science. 2007; 317:783–7. [PubMed: 17615303]
33. Mancuso M, Goddard JM, Erickson D. Nanoporous polymer ring resonators for biosensing. Opt Express. 2012; 20:245–55. [PubMed: 22274347]
34. Safavi-Naeini AH, Chan J, Hill JT, Alegre TPM, Krause A, Painter O. Observation of quantum motion of a nanomechanical resonator. Phys Rev Lett. 2012; 108:33602.
35. Bahl G, Kim KH, Lee W, Liu J, Fan X, Carmon T. Brillouin cavity optomechanics with microfluidic devices. Nat Commun. 2013; 4:1994. [PubMed: 23744103]
36. Hyun Kim K, Bahl G, Lee W, et al. Cavity optomechanics on a microfluidic resonator with water and viscous liquids. Light Sci Appl. 2013; 2:e110.

37. Kim KH, Fan X. Surface sensitive microfluidic optomechanical ring resonator sensors. Appl Phys Lett. 2014; 105:191101.
38. Grilli S, Miccio L, Vespini V, Finizio A, De Nicola S, Ferraro P. Liquid micro-lens array activated by selective electrowetting on lithium niobate substrates. Opt Express. 2008; 16:8084–93. [PubMed: 18545521]
39. Tang SKY, Stan CA, Whitesides GM. Dynamically reconfigurable liquid-core liquid-cladding lens in a microfluidic channel. Lab Chip. 2008; 8:395–401. [PubMed: 18305856]
40. Mao X, Lin S-CS, Lapsley MI, Shi J, Juluri BK, Huang TJ. Tunable liquid gradient refractive index (L-GRIN) lens with two degrees of freedom. Lab Chip. 2009; 9:2050–8. [PubMed: 19568674]
41. Song C, Nguyen NT, Yap YF, Luong TD, Asundi AK. Multi-functional, optofluidic, in-plane, bi-concave lens: tuning light beam from focused to divergent. Microfluid Nanofluid. 2010; 10:671–8.
42. Shi J, Stratton Z, Lin SCS, Huang H, Huang TJ. Tunable optofluidic microlens through active pressure control of an air-liquid interface. Microfluid Nanofluid. 2009; 9:313–8.
43. Yang Y, Chin LK, Tsai JM, Tsai DP, Zheludev NI, Liu AQ. Transformation optofluidics for large-angle light bending and tuning. Lab Chip. 2012; 12:3785–90. [PubMed: 22868356]
44. Parks JW, Cai H, Zempoaltecatl L, et al. Hybrid optofluidic integration. Lab Chip. 2013; 13:4118–23. [PubMed: 23969694]
45. Testa G, Persichetti G, Sarro PM, Bernini R. A hybrid silicon-PDMS optofluidic platform for sensing applications. Biomed Opt Express. 2014; 5:417–26. [PubMed: 24575337]
46. Parks JW, Olson MA, Kim J, et al. Integration of programmable microfluidics and on-chip fluorescence detection for biosensing applications. Biomicrofluidics. 2014; 8:54111.
47. Schudel BR, Choi CJ, Cunningham BT, Kenis PJA. Microfluidic chip for combinatorial mixing and screening of assays. Lab Chip. 2009; 9:1676–80. [PubMed: 19495449]
48. Kim J, Kang M, Jensen EC, Mathies RA. Lifting gate polydimethylsiloxane microvalves and pumps for microfluidic control. Anal Chem. 2012; 84:2067–71. [PubMed: 22257104]
49. Cai H, Parks JW, Wall TA, et al. Optofluidic analysis system for amplification-free, direct detection of Ebola infection. Sci Rep. 2015; 5:14494. [PubMed: 26404403]
50. Zhu H, Sencan I, Wong J, Dimitrov S, Tseng D, Nagashima K, et al. Cost-effective and rapid blood analysis on a cell-phone. Lab Chip. 2013; 13:1282–8. [PubMed: 23392286]
51. Wei Q, Qi H, Luo W, et al. Fluorescent imaging of single nano particles and viruses on a smart phone. ACS Nano. 2013; 7:9147–55. [PubMed: 24016065]
52. Mudanyali O, Dimitrov S, Sikora U, Padmanabhan S, Navruz I, Ozcan A. Integrated rapid-diagnostic-test reader platform on a cellphone. Lab Chip. 2012; 12:2678–86. [PubMed: 22596243]
53. Jiang L, Mancuso M, Lu Z, Akar G, Cesarman E, Erickson D. Solar thermal polymerase chain reaction for smartphone-assisted molecular diagnostics. Sci Rep. 2014; 4:4137. [PubMed: 24553130]
54. Yang W, Conkey DB, Wu B, Yin D, Hawkins AR, Schmidt H. Atomic spectroscopy on a chip. Nat Photonics. 2007; 1:331–5.
55. Wu B, Hulbert JF, Lunt EJ, Hurd K, Hawkins AR, Schmidt H. Slow light on a chip via atomic quantum state control. Nat Photonics. 2010; 4:776–9.
56. Scholten K, Fan X, Zellers ET. A microfabricated optofluidic ring resonator for sensitive, high-speed detection of volatile organic compounds. Lab Chip. 2014; 14:3873–80. [PubMed: 25131718]
57. Collin WR, Scholten KW, Fan X, Paul D, Kurabayashi K, Zellers ET. Polymer-coated micro-optofluidic ring resonator detector for a comprehensive two-dimensional gas chromatographic microsystem: μGC × μGC-μOFRR. Analyst. 2015; 141:261–9. [PubMed: 26588451]
58. Van de Hulst, HC. Light Scattering by Small Particles. New York: Dover Publications; 1957.
59. Domachuk P, Cronin-Golomb M, Eggleton BJ, Mutzenich S, Rosengarten G, Mitchell A. Application of optical trapping to beam manipulation in optofluidics. Opt Express. 2005; 13:7265–75. [PubMed: 19498750]
60. Erickson, D., Li, B., Adleman, JR., Vyawahare, S., Quake, S., Psaltis, D. Spectrographic microfluidic memory. ASME 3rd International Conference on Microchannels and Minichannels; 2005. p. 563-8.

61. Kawata S, Tani T. Optically driven Mie particles in an evanescent field along a channeled waveguide. Opt Lett. 1996; 21:1768–70. [PubMed: 19881795]
62. Gaugiran S, Gétin S, Fedeli JM, et al. Optical manipulation of microparticles and cells on silicon nitride waveguides. Opt Express. 2005; 13:6956–63. [PubMed: 19498716]
63. Gaugiran S, Gétin S, Fedeli JM, Derouard J. Polarization and particle size dependence of radiative forces on small metallic particles in evanescent optical fields. Evidences for either repulsive or attractive gradient forces. Opt Express. 2007; 15:8146–56. [PubMed: 19547141]
64. Néel D, Gétin S, Ferret P, Rosina M, Fedeli JM, Hellesø OG. Optical transport of semiconductor nanowires on silicon nitride waveguides. Appl Phys Lett. 2009; 94:253115.
65. Schmidt BS, Yang AHJ, Erickson D, Lipson M. Optofluidic trapping and transport on solid core waveguides within a microfluidic device. Opt Express. 2007; 15:14322–34. [PubMed: 19550709]
66. Grujic K, Hellesø OG, Hole JP, Wilkinson JS. Sorting of polystyrene microspheres using a Y-branched optical waveguide. Opt Express. 2005; 13:1–7. [PubMed: 19488319]
67. Ulrich R, Kamiya T. Resolution of self-images in planar optical waveguides. J Opt Soc Am. 1978; 68:583–92.
68. Soldano LB, Pennings ECM. Optical multi-mode interference devices based on self-imaging: principles and applications. J Lightwave Technol. 1995; 13:615–27.
69. Cai, H., Poon, AW. Optofluidic microparticle splitters using multimode-interference-based power splitters. Conference on Lasers and Electro-Optics; San Jose, CA: USA. 2012.
70. Hsu L-C, Chen T-C, Yang Y-T, et al. Manipulation of microparticles through optical interference patterns generated by integrated photonic devices. Lab Chip. 2013; 13:1151–5. [PubMed: 23364290]
71. Lin S, Crozier KB. An integrated microparticle sorting system based on near-field optical forces and a structural perturbation. Opt Express. 2012; 20:3367–74. [PubMed: 22418095]
72. Mandal S, Serey X, Erickson D. Nanomanipulation using silicon photonic crystal resonators. Nano Lett. 2010; 10:99–104. [PubMed: 19957918]
73. Van Leest T, Caro J. Cavity-enhanced optical trapping of bacteria using a silicon photonic crystal. Lab Chip. 2013; 13:4358–65. [PubMed: 24057009]
74. Chen Y-F, Serey X, Sarkar R, Chen P, Erickson D. Controlled photonic manipulation of proteins and other nanomaterials. Nano Lett. 2012; 12:1633–7. [PubMed: 22283484]
75. Descharmes N, Perumal Dharanipathy U, Diao Z, Tonin M, Houdré R. Single particle detection, manipulation and analysis with resonant optical trapping in photonic crystals. Lab Chip. 2013; 13:3268–74. [PubMed: 23797114]
76. Little BE, Foresi JS, Steinmeyer G, et al. Ultra-compact Si-SiO_2 microring resonator optical channel dropping filters. IEEE Photonics Technol Lett. 1998; 10:549–51.
77. Chu ST, Little BE, Pan W, Kaneko T, Kokubun Y. Second-order filter response from parallel coupled glass microring resonators. IEEE Photonics Technol Lett. 1999; 11:1426–8.
78. Armani DK, Kippenberg TJ, Spillane SM, Vahala KJ. Ultra-high-Q toroid microcavity on a chip. Nature. 2003; 421:925–8. [PubMed: 12606995]
79. Kippenberg TJ, Spillane SM, Armani DK, Vahala KJ. Fabrication and coupling to planar high-Q silica disk microcavities. Appl Phys Lett. 2003; 83:797–9.
80. Koonath P, Indukuri T, Jalali B. Add-drop filters utilizing vertically coupled microdisk resonators in silicon. Appl Phys Lett. 2005; 86:91102.
81. Cai, H., Poon, AW. Optical manipulation and transport of microparticles on a silicon nitride microracetrack resonator add-drop device. IEEE 7th International Conference on Group IV Photonics; Beijing: China. 2010.
82. Cai H, Poon AW. Optical manipulation and transport of microparticles on silicon nitride microring-resonator-based add-drop devices. Opt Lett. 2010; 35:2855–7. [PubMed: 20808347]
83. Lin S, Crozier KB. Planar silicon microrings as wavelength-multiplexed optical traps for storing and sensing particles. Lab Chip. 2011; 11:4047–51. [PubMed: 22011760]
84. Cai H, Poon AW. Optical manipulation of microparticles using whispering-gallery modes in a silicon nitride microdisk resonator. Opt Lett. 2011; 36:4257–9. [PubMed: 22048383]

85. Soltani M, Lin J, Forties RA, et al. Nanophotonic trapping for precise manipulation of biomolecular arrays. Nat Nanotechnol. 2014; 9:448–52. [PubMed: 24776649]
86. Huang J, Liu X, Zhang Y, Li B. Optical trapping and orientation of *Escherichia coli* cells using two tapered fiber probes. Photon Res. 2015; 3:308–12.
87. Lin S, Crozier KB. Trapping-assisted sensing of particles and proteins using on-chip optical microcavities. ACS Nano. 2013; 7:1725–30. [PubMed: 23311448]
88. Schelle B, Dreß P, Franke H, Klein KF, Slupek J. Physical characterization of lightguide capillary cells. J Phys D Appl Phys. 1999; 32:3157–63.
89. Risk WP, Kim H-C, Miller RD, Temkin H, Gangopadhyay S. Optical waveguides with an aqueous core and a low-index nanoporous cladding. Opt Express. 2004; 12:6446–55. [PubMed: 19488295]
90. Almeida VR, Xu Q, Barrios CA, Lipson M. Guiding and confining light in void nanostructure. Opt Lett. 2004; 29:1209–11. [PubMed: 15209249]
91. Wolfe DB, Conroy RS, Garstecki P, et al. Dynamic control of liquid-core/liquid-cladding optical waveguides. Proc Natl Acad Sci. 2004; 101:12434–8. [PubMed: 15314232]
92. Lim J-M, Kim S-H, Choi J-H, Yang S-M. Fluorescent liquid-core/air-cladding waveguides towards integrated optofluidic light sources. Lab Chip. 2008; 8:1580–5. [PubMed: 18818816]
93. Antonopoulos G, Benabid F, Birks TA, Bird DM, Knight JC, Russell PSJ. Experimental demonstration of the frequency shift of bandgaps in photonic crystal fibers due to refractive index scaling. Opt Express. 2006; 14:3000–6. [PubMed: 19516439]
94. Bernini R, DeNuccio E, Minardo A, Zeni L, Sarro PM. Liquid-core/liquid-cladding integrated silicon ARROW waveguides. Opt Commun. 2008; 281:2062–6.
95. Schmidt H, Hawkins AR. Optofluidic waveguides: I. Concepts and implementations. Microfluid Nanofluid. 2008; 4:3–16. [PubMed: 21442048]
96. Hawkins AR, Schmidt H. Optofluidic waveguides: II. Fabrication and structures. Microfluid Nanofluid. 2008; 4:17–32.
97. Renn MJ, Montgomery D, Vdovin O, Anderson DZ, Wieman CE, Cornell EA. Laser-guided atoms in hollow-core optical fibers. Phys Rev Lett. 1995; 75:3253–6. [PubMed: 10059537]
98. Mandal S, Erickson D. Optofluidic transport in liquid core waveguiding structures. Appl Phys Lett. 2007; 90:184103.
99. Cran-McGreehin S, Krauss TF, Dholakia K. Integrated monolithic optical manipulation. Lab Chip. 2006; 6:1122–4. [PubMed: 16929390]
100. Yang AHJ, Moore SD, Schmidt BS, Klug M, Lipson M, Erickson D. Optical manipulation of nanoparticles and biomolecules in sub-wavelength slot waveguides. Nature. 2009; 457:71–5. [PubMed: 19122638]
101. Duguay MA, Kokubun Y, Koch TL, Pfeiffer L. Antiresonant reflecting optical waveguides in SiO_2-Si multilayer structures. Appl Phys Lett. 1986; 49:13–5.
102. Measor P, Kühn S, Lunt EJ, Phillips BS, Hawkins AR, Schmidt H. Hollow-core waveguide characterization by optically induced particle transport. Opt Lett. 2008; 33:672–4. [PubMed: 18382513]
103. Kühn S, Measor P, Lunt EJ, et al. Loss-based optical trap for on-chip particle analysis. Lab Chip. 2009; 9:2212–6. [PubMed: 19606298]
104. Kühn S, Lunt EJ, Phillips BS, Hawkins AR, Schmidt H. Optofluidic particle concentration by a long-range dual-beam trap. Opt Lett. 2009; 34:2306–8. [PubMed: 19649079]
105. Schmidt, H., Hawkins, AR. All-optical particle trap using two orthogonally intersecting beams. CLEO: 2011– Laser Science to Photonic Applications; 2011.
106. Kühn S, Phillips BS, Lunt EJ, Hawkins AR, Schmidt H. Ultralow power trapping and fluorescence detection of single particles on an optofluidic chip. Lab Chip. 2010; 10:189–94. [PubMed: 20066246]
107. Leake KD, Olson MAB, Ozcelik D, Hawkins AR, Schmidt H. Spectrally reconfigurable integrated multi-spot particle trap. Opt Lett. 2015; 40:5435–8. [PubMed: 26625019]
108. Leake KD, Phillips BS, Yuzvinsky TD, Hawkins AR, Schmidt H. Optical particle sorting on an optofluidic chip. Opt Express. 2013; 21:32605–10. [PubMed: 24514854]

109. Bellini N, Vishnubhatla KC, Bragheri F, et al. Femtosecond laser fabricated monolithic chip for optical trapping and stretching of single cells. Opt Express. 2010; 18:4679–88. [PubMed: 20389480]
110. Estevez MC, Alvarez M, Lechuga LM. Integrated optical devices for lab-on-a-chip biosensing applications. Laser Photonics Rev. 2012; 6:463–87.
111. Measor P, Seballos L, Yin D, et al. On-chip surface-enhanced Raman scattering detection using integrated liquid-core waveguides. Appl Phys Lett. 2007; 90:211107.
112. Wang M, Jing N, Chou I, Cote GL, Kameoka J. An optofluidic device for surface enhanced Raman spectroscopy. Lab Chip. 2007; 7:630–2. [PubMed: 17476383]
113. Zhu H, White IM, Suter JD, Zourob M, Fan X. Optofluidic microring resonator for sensitive label-free viral detection. Analyst. 2008; 133:356–60. [PubMed: 18299750]
114. White IM, Yazdi SH, Yu WW. Optofluidic SERS: synergizing photonics and microfluidics for chemical and biological analysis. Microfluid Nanofluid. 2012; 13:205–16.
115. Yazdi SH, White IM. A nanoporous optofluidic microsystem for highly sensitive and repeatable surface enhanced Raman spectroscopy detection. Biomicrofluidics. 2012; 6:14105. [PubMed: 22291867]
116. Yu WW, White M. Chromatographic separation and detection of target analytes from complex samples using inkjet printed SERS substrates. Analyst. 2013; 138:3679–86. [PubMed: 23671906]
117. Wu HY, Cunningham BT. Point-of-care detection and real-time monitoring of intravenously delivered drugs via tubing with an integrated SERS sensor. Nanoscale. 2014; 6:5162–71. [PubMed: 24699532]
118. Huang MC, Galarreta BE, Cetin A, Altug H. Actively transporting virus like analytes with optofluidics for rapid and ultrasensitive biodetection. Lab Chip. 2013; 13:4841–7. [PubMed: 24170146]
119. Escobedo C, Brolo AG, Gordon R, Sinton D. Optofluidic concentration: plasmonic nanostructure as concentrator and sensor. Nano Lett. 2012; 12:1592–6. [PubMed: 22352888]
120. Arnold S, Dantham VR, Barbre C, Garetz BA, Fan X. Periodic plasmonic enhancing epitopes on a whispering gallery mode biosensor. Opt Express. 2012; 20:26147–59. [PubMed: 23187470]
121. Barik A, Otto LM, Yoo D, Jose J, Johnson TW, Oh S-H. Dielectrophoresis-enhanced plasmonic sensing with gold nanohole arrays. Nano Lett. 2014; 14:2006–12. [PubMed: 24646075]
122. Chang T-Y, Huang M, Yanik AA, et al. Large-scale plasmonic microarrays for label-free high-throughput screening. Lab Chip. 2011; 11:3596–602. [PubMed: 21901194]
123. Coskun AF, Cetin AE, Galarreta BC, Alvarez DA, Altug H, Ozcan A. Lensfree optofluidic plasmonic sensor for real-time and label-free monitoring of molecular binding events over a wide field-of-view. Sci Rep. 2014; 4:6789. [PubMed: 25346102]
124. Zeng B, Gao YJ, Bartoli F. Differentiating surface and bulk interactions in nanoplasmonic interferometric sensor arrays. Nanoscale. 2015; 7:166–70. [PubMed: 25407985]
125. Kumar K, Dahlin AB, Sannomiya T, Kaufmann S, Isa L, Reimhult E. Embedded plasmonic nanomenhirs as location-specific biosensors. Nano Lett. 2013; 13:6122–9. [PubMed: 24188470]
126. Mazzotta F, Johnson TW, Dahlin AB, Shaver J, Oh S-H, Höök F. Influence of the evanescent field decay length on the sensitivity of plasmonic nanodisks and nanoholes. ACS Photonics. 2015; 2:256–62.
127. Adato R, Altug H. In-situ ultra-sensitive infrared absorption spectroscopy of biomolecule interactions in real time with plasmonic nanoantennas. Nat Commun. 2013; 4:2154. [PubMed: 23877168]
128. Oh B-R, Huang N-T, Chen W, et al. Integrated nanoplasmonic sensing for cellular functional immunoanalysis using human blood. ACS Nano. 2014; 8:2667–76. [PubMed: 24568576]
129. Cetin AE, Altug H. Fano resonant ring/disk plasmonic nanocavities on conducting substrates for advanced biosensing. ACS Nano. 2012; 6:9989–95. [PubMed: 23092386]
130. Gao Y, Xin Z, Gan Q, Cheng X, Bartoli FJ. Plasmonic interferometers for label-free multiplexed sensing. Opt Express. 2013; 21:5859–71. [PubMed: 23482154]
131. Cetin AE, Coskun AF, Galarreta BC, et al. Handheld high-throughput plasmonic biosensor using computational on-chip imaging. Light Sci Appl. 2014; 3:e122.

132. Rodrigo D, Limaj O, Janner D, et al. Mid-infrared plasmonic biosensing with graphene. Science. 2015; 349:165–8. [PubMed: 26160941]
133. Daaboul A, Zhang X, Hwang GM, Goldberg BB, Ünlü MS. High-throughput detection and sizing of individual low-index nanoparticles and viruses for pathogen identification. Nano Lett. 2014; 14:4727.
134. Mudanyali O, McLeod E, Luo W, et al. Wide-field optical detection of nanoparticles using on-chip microscopy and self-assembled nanolenses. Nat Photonics. 2013; 7:247–54.
135. Faez S, Lahini Y, Weidlich S, et al. Fast, label-free tracking of single viruses and weakly scattering nanoparticles in a nanofluidic optical fiber. ACS Nano. 2015; 9:12349–57. [PubMed: 26505649]
136. Lien V, Berdichevsky Y, Lo Y-H. A prealigned process of integrating optical waveguides with microfluidic devices. IEEE Photonics Technol Lett. 2004; 16:1525–7.
137. Lien V, Zhao K, Berdichevsky Y, Lo Y-H. High-sensitivity cytometric detection using fluidic-photonic integrated circuits with array waveguides. IEEE J Select Top Quantum Electron. 2005; 11:827–34.
138. Bliss CL, McMullin JN, Backhouse CJ. Rapid fabrication of a microfluidic device with integrated optical waveguides for DNA fragment analysis. Lab Chip. 2007; 7:1280–7. [PubMed: 17896011]
139. Yin D, Barber JP, Hawkins AR, Deamer DW, Schmidt H. Integrated optical waveguides with liquid cores. Appl Phys Lett. 2004; 85:3477–9.
140. Schmidt H, Yin D, Barber JP, Hawkins AR. Hollow-core waveguides and 2D waveguide arrays for integrated optics of gases and liquids. IEEE J Select Top Quantum Electron. 2005; 11:519–27.
141. Bernini R, Campopiano S, Zeni L, Sarro PM. ARROW optical waveguides based sensors. Sens Actuators B Chem. 2004; 100:143–6.
142. Yin D, Deamer DW, Schmidt H, Barber JP, Hawkins AR. Single-molecule detection sensitivity using planar integrated optics on a chip. Opt Lett. 2006; 31:2136–8. [PubMed: 16794704]
143. Yin D, Lunt EJ, Rudenko MI, Deamer DW, Hawkins AR, Schmidt H. Planar optofluidic chip for single particle detection, manipulation, and analysis. Lab Chip. 2007; 7:1171–5. [PubMed: 17713616]
144. Yin D, Lunt EJ, Barman A, Hawkins AR, Schmidt H. Microphotonic control of single molecule fluorescence correlation spectroscopy using planar optofluidics. Opt Express. 2007; 15:7290–5. [PubMed: 19547052]
145. Zhao Y, Jenkins M, Measor P, et al. Hollow waveguides with low intrinsic photoluminescence fabricated with Ta_2O_5 and SiO_2 films. Appl Phys Lett. 2011; 98:91104. [PubMed: 21448254]
146. Parks JW, Wall TA, Cai H, Hawkins AR, Schmidt H. Enhancement of ARROW photonic device performance via thermal annealing of PECVD-based SiO_2 waveguides. IEEE J Select Top Quantum Electron. 2016; 22:1–6.
147. Zhao Y, Leake KD, Measor P, et al. Optimization of interface transmission between integrated solid core and optofluidic waveguides. IEEE Photonics Technol Lett. 2012; 24:46–8.
148. Ozcelik D, Parks JW, Wall TA, et al. Optofluidic wavelength division multiplexing for single-virus detection. Proc Natl Acad Sci. 2015; 112:12933–7. [PubMed: 26438840]
149. Kiesel P, Bassler M, Beck M, Johnson N. Spatially modulated fluorescence emission from moving particles. Appl Phys Lett. 2009; 94:41107.
150. Martini J, Recht MI, Huck M, Bern MW, Johnson NM, Kiesel P. Time encoded multicolor fluorescence detection in a microfluidic flow cytometer. Lab Chip. 2012; 12:5057–62. [PubMed: 23044636]
151. Ozcelik D, Stott MA, Parks JW, et al. Signal-to-noise enhancement in optical detection of single viruses with multispot excitation. IEEE J Select Top Quantum Electron. 2016; 22:6–11.
152. Dekker C. Solid-state nanopores. Nat Nanotechnol. 2007; 2:209–15. [PubMed: 18654264]
153. Liu S, Zhao Y, Parks JW, Deamer DW, Hawkins AR, Schmidt H. Correlated electrical and optical analysis of single nanoparticles and biomolecules on a nanopore-gated optofluidic chip. Nano Lett. 2014; 14:4816–20. [PubMed: 25006747]

154. Liu S, Wall TA, Ozcelik D, Parks JW, Hawkins AR, Schmidt H. Electro-optical detection of single λ-DNA. Chem Commun. 2015; 51:2084–7.

155. Liu S, Hawkins AR, Schmidt H. Optofluidic devices with integrated solid-state nanopores. Microchim Acta. 2016; 183:1275–87.

156. Parks JW, Schmidt H. Flexible optofluidic waveguide platform with multi-dimensional reconfigurability. Sci Rep. 2016; 6:33008. [PubMed: 27597164]

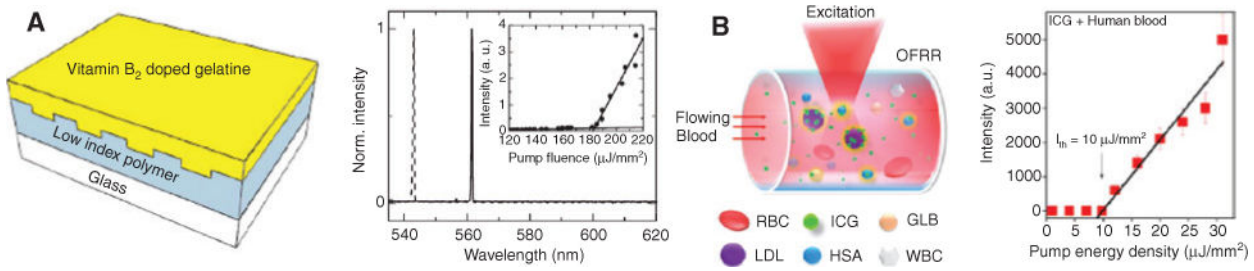

Figure 1.

Bioinspired optofluidic laser sources.

(A) Left: schematic view of DFB laser with vitamin-doped gelatin layer as active medium; right: corresponding lasing spectrum (inset: L-I curve) showing single-mode emission under optical pumping (after [24]). (B) Left: schematic view of optically pumped “blood laser” realized in OFRR illustrating components in serum (GLB, globulins; HAS, human serum albumin; ICG, active dye medium; WBC, white blood cells); right: corresponding L-I curve under optical pumping (after [27]).

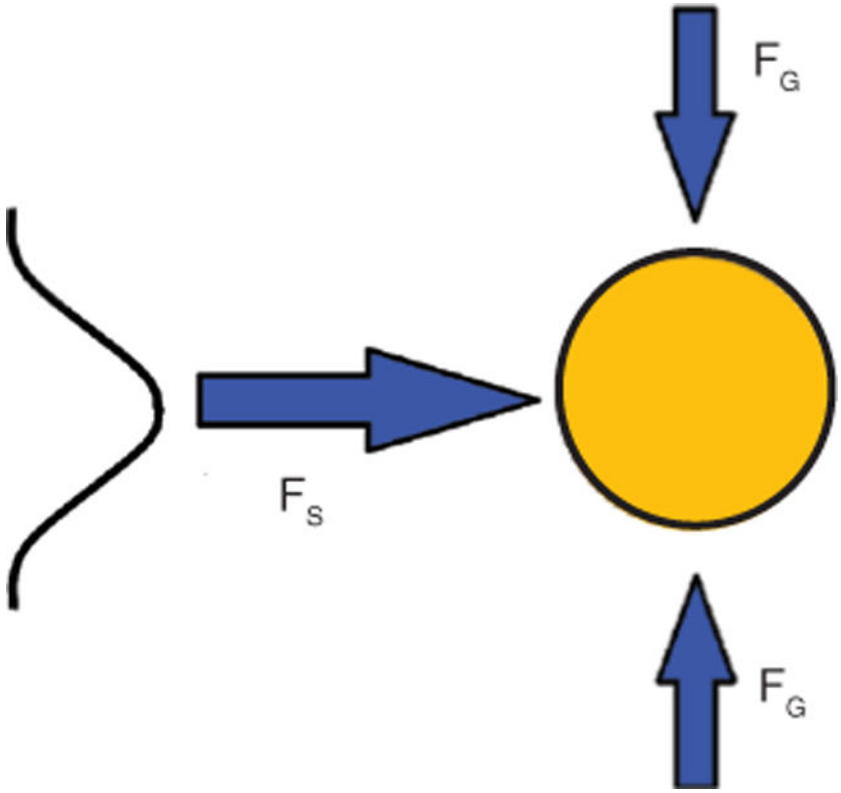

Figure 2.

Optical forces on dielectric particle generated by a Gaussian beam.

For typical conditions (the particle index is larger than that of surrounding medium), the beam generates a scattering force F_S along the light propagation direction and a gradient force F_G pulling the particle toward the high-intensity regions.

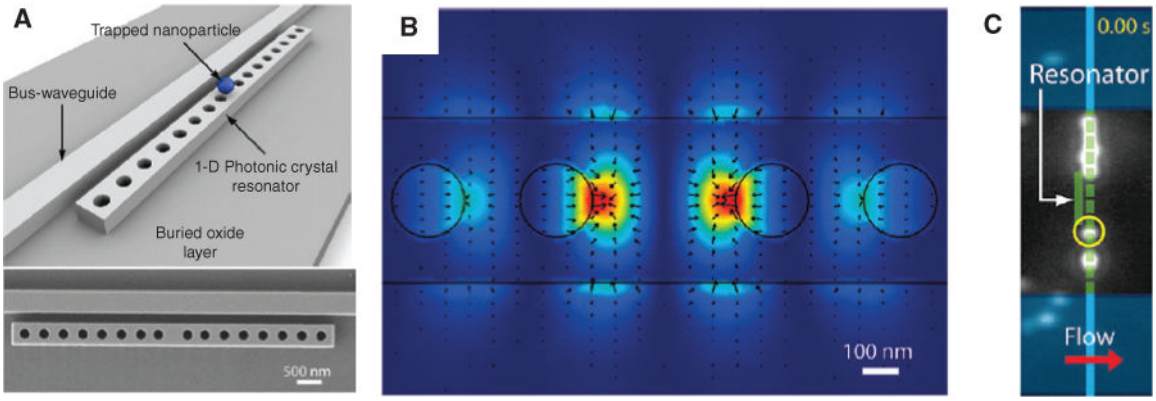

Figure 3.

Photonic crystal resonator for on-chip particle trapping.

(A) Schematic (top) and SEM (bottom) of 1D optofluidic photonic crystal resonator. (B) 3D FEM simulation showing strong field confinement within the 1D resonator cavity (red color indicates large forces). Black ARROWs: direction and magnitude of the optical forces. (C) 500 nm polystyrene particle (yellow circle) trapped on top of the waveguide [72].

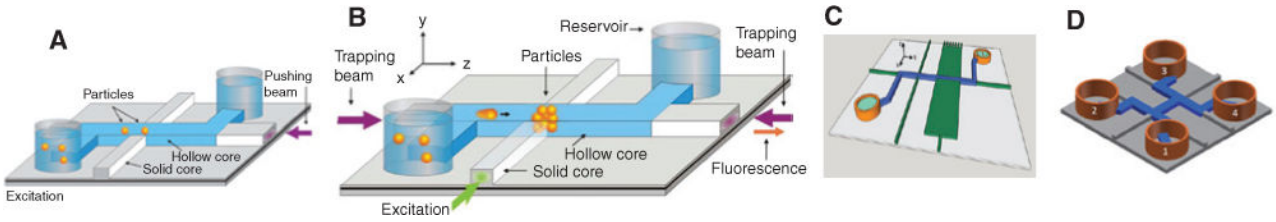

Figure 4.

Schematic of liquid-core ARROW chips: (A) used for pushing [101], (B) used for trapping and detection [102], (C) used for multiparticle trapping [107], and (D) used for sorting [108].

Blue channels indicate liquid-core waveguides carrying microscale and nanoscale particles and gray/green channels show solid-core waveguides.

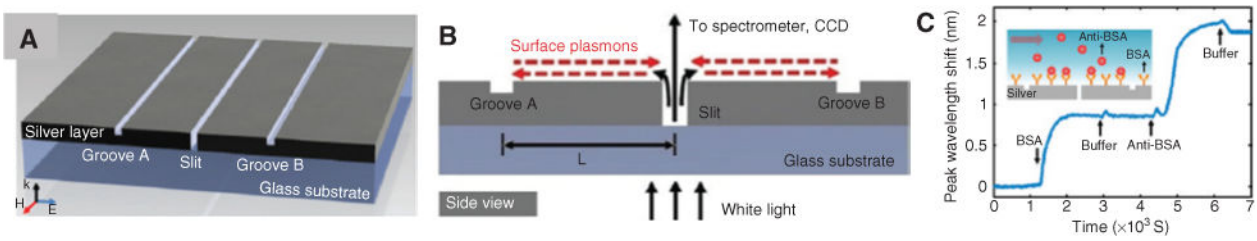

Figure 5.

Plasmonic biosensor [130].

(A) Schematic of the plasmonic interferometer based on nanoscale slits and grooves in silver film. (B) Side view of the interferometer structure showing interference between directly transmitted light and surface plasmons reflected at grooves to create index-dependent transmission signal. (C) Time-dependent sensor response upon BSA adsorption to the sensor surface and subsequent specific protein binding between BSA and anti-BSA.

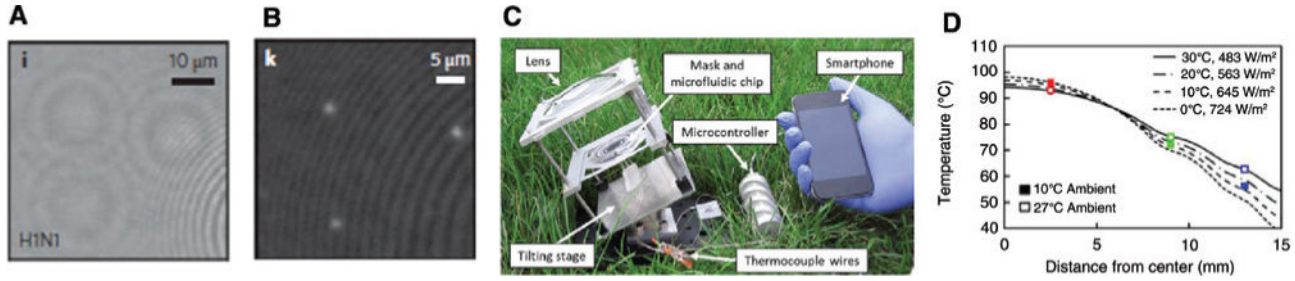

Figure 6.

Lensfree pixel super-resolved holographic detection of individual influenza A (H1N1) viruses.

(A) Lensfree super-resolved holographic image and (B) lensfree phase reconstruction (after [134]). (C) Bench-top component for solar-assisted PCR holding lens, PCR chip, and a rotational stage. (D) Simulations showing thermal profiles across microfluidic disk for carrying out PCR (after [53]).

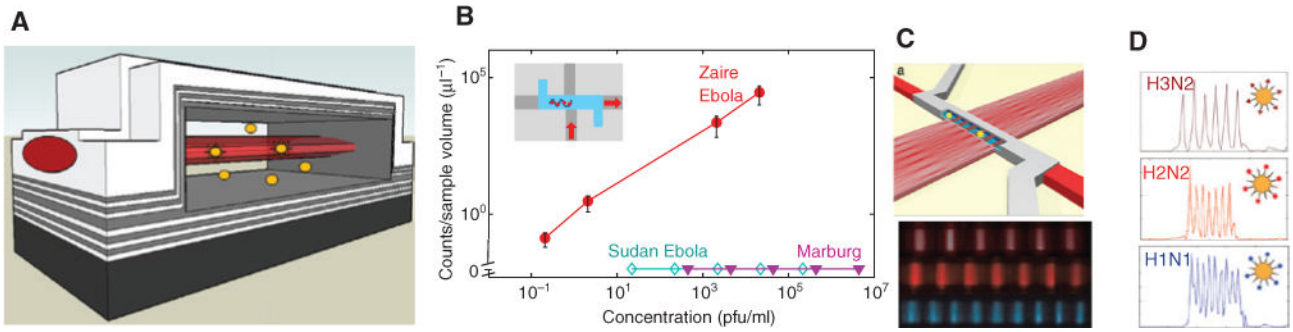

Figure 7.

Optofluidic bioanalysis with liquid-core ARROW devices.

(A) Schematic view of the intersection of liquid- and solid-core waveguides in which target particles are excited by a traversing optical mode in a femtoliter volume. (B) Concentration-dependent detection of single viral nucleic acids on ARROW chip with high specificity (inset: top-down view of chip layout; adapted from [48]). (C) Optofluidic wavelength division multiplexing: MMI waveguide creates multispot pattern in fluidic channel; bottom: experimental observation of distinct spot patterns at three different wavelengths. (D) Multiplex detection of three influenza subtypes using MMI multispot excitation; each trace originates from a single virus particle (after [148]).